Mix Hydrate formation by CH4-CO2 exchange using Phase Field Theory with implicit Thermodynamics

M. Qasim, K. Baig, B. Kvamme and J. Bauman

***Abstract*—** Natural gas hydrates are ice-like structures composed of water and gas (mostly methane) molecules. They are found worldwide and contain huge amounts of bound methane. Therefore, it represent potentially vast and yet untapped energy resources. Hydrates from carbon dioxide are thermodynamically more stable than methane hydrate over large regions of condition. Mixed hydrates of structure I, in which methane occupies the small cavities are more stable than methane hydrate over all ranges of pressures and temperatures. The exchange of originally bound methane in hydrate with carbon dioxide is a great way to achieve two goals, the in situ release of hydrocarbon gas and a cleaner environment through safe storage of carbon dioxide. The resulting hydrate is a mix. Carbon dioxide can only replace methane in large cavities due to its size and therefore it forms mix methane-carbon dioxide hydrate with methane in the small cavities and a maximum theoretical exchange of 75% of the in situ methane. An improved thermodynamic model is implicitly implemented in phase field theory to study the kinetic rates due to the exchange process. A thin layer of water between methane hydrate and carbon dioxide is implemented in addition to the initial methane for a more realistic representation of a reservoir situation in which hydrate saturation is always lower than 100%. The nucleation on water-carbon dioxide interface is expected to be very slow compared to the growth rate. To trigger the carbon dioxide hydrate formation four small regions of carbon dioxide hydrate are placed on the water-carbon dioxide interface. The exchange process involves an initial dissociation of methane hydrate and the carbon dioxide will start forming hydrate. In term of Gibbs phase rule the system can theoretically reach equilibrium as limit if pressure and temperature is defined and the final hydrate is uniform. On the other hand the limited size of the system and the initial balance of masses of the three components methane, carbon dioxide and water will not make equilibrium possible in the model system. This implies also that kinetic rates of hydrate formation, hydrate reformation and dissociation will depend on composition of surrounding phases and corresponding free energies. This is also the expected situation in a porous media like a hydrate reservoir, in which the hydrate is in a stationary balance with fluids and typically kept trapped by layers of clay or shale. Phase field theory is a tool for evaluation of kinetic rates of different phase transitions as well as the relative impact of thermodynamic control and mass transport control. Heat transport is very rapid compared to mass transport and is neglected in this work.

***Keywords*—**Phase field theory, Natural gas hydrate, Hydrodynamics, Hydrate exchange.

I. Introduction

Gas hydrates are ice-like substances of water molecules encaging gas molecules called guest. Natural gas hydrates are dominated by methane and most naturally occurring hydrates are formed from biogenic sources. They form under high pressure and low temperature conditions within the upper hundred meters of the sub-seabed sediments [1]. Gas hydrate mostly exist in two crystalline structures structure I (sI) and structure II (sII). There may also rarely found a third type structure H denoted as sH. These structures vary in composition and types of cavities that constitutes the hydrate structure depending on the size of the guest molecule. The scope of this work is on hydrates with carbon dioxide (CO2) and methane (CH4) as guests. These two components both form the structure I hydrate and special focus will therefore be on this particular structure. Using the explanation by Sloan [22], structure I is a cubic crystalline in shape and formed with guest molecules having diameter between 4.2 and 6 Å, such as methane, carbon dioxide, ethane and hydrogen sulfide. One unit cell in it consists of 46 water molecules. It has two small and six large cages in one unit cell. The small cage has the shape of a 12 sided cavity with 12 pentagonal faces in each side and called pentagonal dodecahedron (5^{12}). The large cage has the shape of a 14 sided cavity (with 12 pentagonal faces and 2 hexagonal) faces and called tetradecahedron ($5^{12}6^2$). If all the cavities are filled with guest molecules the mole percent of water would be about 85%. Normally, not all cavities may found be completely occupied with guest molecules. Due to this very high water content hydrates look like snow or ice. They are also sometimes called as 'ice that burns' as shown in Fig. 1. It is natural to assume that hydrate properties may little depend on guest molecules due to their low content, but it is not the case. The most

Paper submitted November 25, 2011: Revised version submitted January 02, 2012. This work was supported financially by The Research Council of Norway through the projects: "subsurface storage of CO2 – Risk assessment, monitoring and remediation", Project number: 178008/I30, FME – SUCCESS, Project number: 804831, "CO2 injection for extra production", Project number: 801445, PETROMAKS project Gas hydrates on the Norwegian-Barents Sea-Svalbard margin (GANS, Norwegian Research Council) Project number: 175969/S30 and INJECT "subsurface storage of CO2", Project number: 805173.

M. Qasim, is with the University of Bergen, Post box 7800, 5020 Bergen, Allegt. 55 Norway. (e-mail: Muhammad.Qasim@ift.uib.no).

K. Baig, is with the University of Bergen, Post box 7800, 5020 Bergen, Allegt. 55 Norway. (e-mail: kba062@ift.uib.no).

B. kvamme[1], is with the University of Bergen, Post box 7800, 5020 Bergen, Allegt. 55 Norway (phone: +47-555-83310; e-mail: Bjorn.Kvamme@ift.uib.no).

J. Bauman is with the University of Bergen, Post box 7800, 5020 Bergen, Allegt. 55 Norway. (e-mail: Jordan.Bauman@ift.uib.no).

striking property of hydrate is that they can be formed and exist at temperatures higher than 0^0C if the pressure is high enough.

Fig.1 'Ice that burns', (Photo courtesy of: J. Pinkston and L. Stern / Us Geological Survey).

These gas hydrates are widely distributed in sediments along continental margins, and harbor enormous amounts of energy. Massive hydrates that outcrop the sea floor have been reported in the Gulf of Mexico [2]. Hydrate accumulations have also been found in the upper sediment layers of Hydrate ridge, off the coast of Oregon and a fishing trawler off Vancouver Island recently recovered a bulk of hydrate of approximately 1000kg [3]. Håkon Mosby Mud Volcano of Bear Island in the Barents Sea with hydrates is openly exposed at the ocean floor [4]. These are only few examples of the worldwide evidences of unstable hydrate occurrences that leaks methane to the oceans and eventually may be a source of methane increase in the atmosphere.

Hydrates of methane are not thermodynamically stable at mineral surfaces. From a thermodynamic point of view the reason is simply that water structure on hydrate surfaces are not able to obtain optimal interactions with surfaces of calcite, quarts and other reservoir minerals. The impact of this is that hydrates are separated from the mineral surfaces by fluid channels. The sizes of these fluid channels are not known and are basically not even unique in the sense that it depends on the local fluxes of all fluids in addition to the surface thermodynamics. Stability of natural gas hydrate reservoirs therefore depends on sealing or trapping mechanisms similar to ordinary oil and gas reservoirs. Many hydrate reservoirs are in a dynamic state where hydrate is leaking from top by contact with groundwater/seawater which is under saturated with respect to methane and new hydrates form from deeper gas sources.

Global energy needs and climate stress from greenhouse gases require new sources of energy and the management of CO2 emissions. Natural gas hydrate provides a great solution being a potential source of energy and reduction of CO2 emissions. Methane can be recovered by number of ways like depressurization, heating and injection of another gas. The scope of this work deals with the kinetic rates of CO2 injection into methane hydrate. This process is a favorable way to store a greenhouse gas (CO2) for long period of time and enables the ocean floor to remain stabilized even after recovering the methane gas [10]. Because, of the size CO2 can only fit into large cavities and it will force methane in large cavities to release. This exchange is a solid phase exchange and therefore in result the new hydrate formed is a mix CO2/CH4 hydrate which is thermodynamically more stable than CH4 hydrate over substantial regions of pressure and temperature.

Gas hydrates have great capacity to store gases [5-7] and several investigations of potential for using hydrate phase for storage and transport have been conducted even though the hydrates are not stable when exposed to new surroundings like for instance air. The storage of CO2 in reservoirs has already been established as a feasible alternative for reducing CO2 emissions into the atmosphere. Injection of produced CO2 from Sleipner oil and gas field into the Utsira formation was the first industrial CO2 aquifer storage project. A number of studies conducted for the Utsira storage. See for instance Xu and Preuss [8] and references therein. There are regions in the northern parts of North Sea and the Barents Sea suitable for CO2 storage which contains regions of pressure and temperature conditions which are within the CO2 hydrate stability regions. Kinetic rates for CO2 hydrate formation, as well as dissociation of CO2 hydrate towards under saturated water is therefore important in reservoir modeling of CO2 storage in those regions. There are also natural gas hydrates in those regions and storing CO2 in natural gas hydrate reservoirs may provide a win-win situation of safe long term CO2 storage in the form of hydrate and simultaneous release of natural gas.

In our studies we are more interested in the type of CO2 storage provided by the reservoirs that already contains natural gas hydrates. Mixed CO2 and methane hydrate, in which methane fills some portion of the small cavities, is significantly more stable than natural gas hydrates. Injecting CO2 into in situ natural hydrate results in the formation of CO2 hydrate by naturally replacing the originally bounded in-situ hydrocarbons and therefore, at the same time releases the hydrocarbons. ConocoPhillips has currently in May 2012 has completed working on a field trial on the Alaska North Slope together with the US Department of Energy (DOE project MH-06553) as a major funding agency for the project. Now they are focusing in evaluating the extensive test data. It is believed that the data achieved by this trial will be helpful to experimentally justify the theoretical works like the one presented in this article. The aim is to investigate the release methane through CO2 injection.

Theoretically, Phase field theory is the main tool to give a deep understanding into the kinetic rates involved during this exchange. This work has used the modified Phase Field Theory as illustrated by Qasim et al. [9]. This process strongly depends on the accurate thermodynamic model and therefore an improved thermodynamic model as in [15] is implemented along with modified Phase Field Theory.

II. Phase Field Model

Phase field theory model follows the formulation of

Wheeler et al. [11], which historically has been mostly applied to descriptions of the isothermal phase transition between ideal binary-alloy liquid and solid phases of limited density differences. The hydrodynamics effects and variable density were incorporated in a three components phase field theory by Kvamme et al. [12] through implicit integration of Navier stokes equation following the approach of Qasim et al.[9]. The phase field parameter ϕ is an order parameter describing the phase of the system as a function of spatial and time coordinates. The phase field parameter ϕ is allowed to vary continuously from 0 to 1 on the range from solid to liquid.

The solid state is represented by the hydrate and the liquid state represents fluid and aqueous phase. The solidification of hydrate is described in terms of the scalar phase field $\phi(x_1, x_2, x_3)$ where x_1, x_2, x_3 represents the molar fractions of CH4, CO2 and H2O respectively with obvious constraint on conservation of mass $\sum_{i=1}^{3} x_i = 1$. The field ϕ is a structural order parameter assuming the values $\phi = 0$ in the solid and $\phi = 1$ in the liquid [13]. Intermediate values correspond to the interface between the two phases. The starting point of the three component phase field model is a free energy functional [12],

$$F = \int d\underline{r} \left(\frac{\varepsilon_\phi^2}{2} T(\nabla\phi)^2 + \sum_{i,j=1}^{3} \frac{\varepsilon_{xi,j}^2}{4} T\rho\left(x_i \nabla x_j - x_j \nabla x_i\right)^2 + f_{bulk}(\phi, x_1, x_2, x_3, T) \right), \quad (1)$$

which is an integration over the system volume, while the subscripts i, j represents the three components, ρ is molar density depending on relative compositions, phase and flow. The bulk free energy density described as

$$f_{bulk} = WTg(\phi) + \left(1 - p(\phi)\right) f_S(x_1, x_2, x_3, T) + p(\phi) f_L(x_1, x_2, x_3, T) . \quad (2)$$

The phase field parameter switches on and off the solid and liquid contributions f_S and f_L through the function $p(\phi) = \phi^3(10 - 15\phi + 6\phi^2)$, and note that $p(0) = 0$ and $p(1) = 1$. This function was derived from density functional theory studies of binary alloys and has been adopted also for our system of hydrate phase transitions. The binary alloys are normally treated as ideal solutions. The free energy densities of solid and liquid is given by

$$f_S = G_S \rho_m^{hyd} , \quad (3)$$

$$f_L = G_L \rho_m^{L} . \quad (4)$$

The details of densities ρ_m^{hyd} and ρ_m^{L} can be found in Qasim et al. [14]. The hydrate free energy away from equilibrium G_S is calculated using the following equation:

$$G_S = G^{EQ} + \sum_r^{r=m,c,w} \frac{\partial G_S}{\partial x_r} dx_r + \frac{\partial G_S}{\partial P} dP + \frac{\partial G_S}{\partial T} dT . \quad (5)$$

Here G^{EQ} is the free energy at equilibrium. The free energy gradients with respect to mole fraction, pressure and temperature are $\frac{\partial G_S}{\partial x_r}$, $\frac{\partial G_S}{\partial P}$ and $\frac{\partial G_S}{\partial T}$ respectively. Where subscript r represents any of the components of the hydrate: methane, carbon dioxide and methane. The detail calculations of the free energy gradients can be found in Kvamme et al. [15]. The free energy of the liquid G_L is discussed in the following fluid and aqueous thermodynamic section.

The function $g(\phi) = \phi^2(1 - \phi^2)/4$ ensures a double well form of the f_{bulk} with a free energy scale $W = \left(1 - \frac{x_i}{v_m}\right) W_A + \frac{x_i}{v_m} W_B$ with $g(0) = g(1) = 0$, where v_m is the average molar volume of water. In order to derive a kinetic model we assume that the system evolves in time so that its total free energy decreases monotonically [13].

The usual equations of motion are supplemented with appropriate convection terms as explained by Tegze et al [16]. Given that the phase field is not a conserved quantity, the simplest form for the time evolution that ensures a minimization of the free energy is

$$\frac{\partial \phi}{\partial t} + (\vec{v}.\nabla)\phi = -M_\phi(\phi, x_1, x_2, x_3) \frac{\delta F}{\delta \phi} , \quad (6)$$

$$\frac{\partial x_i}{\partial t} + (\vec{v}.\nabla)x_i = \nabla.\left(M_{xi}(\phi, x_1, x_2, x_3) \nabla \frac{\delta F}{\delta xi}\right) , \quad (7)$$

where $\vec{v}$ is the velocity, $M_{xi} = x_i(1 - x_i)\frac{1}{RT} D$ and $M_\phi = \left(1 - \frac{x_i}{v_m}\right) M^A + \frac{x_i}{v_m} M^B$ are the mobilities associated with coarse-grained equation of motion which in turn are related to their microscopic counter parts. Where $D = D_S + (D_L - D_S)p(\phi)$ is the diffusion coefficient. The details are given elsewhere [12].

An extended phase field model is formulated to account for the effect of fluid flow, density change and gravity. This is achieved by coupling the time evolution with the Navier Stokes Equations. The phase and concentration fields associates hydrodynamic equation as described by Conti [17-19]

$$\frac{\partial \rho}{\partial t} = -\rho_m \nabla.\vec{v}, \qquad \rho \frac{\partial \vec{v}}{\partial t} + \rho(\vec{v}.\nabla)\vec{v} = \rho\vec{g} + \nabla.P. \quad (8)$$

Where $\vec{g}$ is the gravitational acceleration. ρ_m is the density of the system in hydrate (ρ_m^{Hyd}) and liquid (ρ_m^{L}). The detail for calculating these densities are already given by Qasim et al [14]. Further

$$P = \xi + \Pi. \quad (9)$$

is the generalization of stress tensor [17-20], ξ represents

non-dissipative part and Π represents the dissipative part of the stress tensor.

III. Fluid Thermodynamics

The free energy of the fluid phase is assumed to have

$$G_L = \sum_{i=1}^{3} x_i \mu_i^{Fluid}, \quad (11)$$

where μ_i^{Fluid} is the chemical potential of the ith component. The solubility of water is assumed to follow the Raoult's law. The lower concentration of water in the fluid phase and its corresponding minor importance for the thermodynamics results in the following form of water chemical potential with some approximation of fugacity and activity coefficient:

$$\mu_3^{Fluid} = \mu_3^{\infty} + RTln(y_3), \quad (12)$$

where μ_3^{∞} chemical potential of water at infinite dilution and y_3 is the mole fraction of water in the fluid phase. The chemical potential for the mixed fluid states is approximated as

$$\mu_i^{Fluid} = \mu_i^{SRK,pure} + RTln(y_3), \quad (13)$$

where i represents CH4 or CO2. The details are available in Svandal et al. [21].

IV. Aqueous Thermodynamics

The free energy of the aqueous phase assumed as

$$G_L = \sum_{i=1}^{3} x_i \mu_i^{aqueous}, \quad (14)$$

the chemical potential $\mu_i^{aqueous}$ of aqueous phase has the general form derived from excess thermodynamics

$$\mu_3^{H} = \mu_i^{\infty} + RTln(x_i \gamma_i^{\infty}) + v_i(P - P_0). \quad (15)$$

μ_i^{∞} is the chemical potential of component i in water at infinite dilution, γ_i^{∞} is the activity coefficient of component i in the aqueous solution in the asymmetric convention (γ_i^{∞} approaches unity in the limit of x becoming infinitely small). The chemical potentials at infinite dilution as a function of temperature are found by assuming equilibrium between fluid and aqueous phases$\left(\mu_3^{Fluid} = \mu_3^{aqueous}\right)$. This is done at low pressures where the solubility is very low, using experimental values for the solubility and extrapolating the chemical potential down to a corresponding value for zero concentration. The activity coefficient can be regressed by using the model for equilibrium to fit experimental solubility data. The chemical potential of water can be written as:

$$\mu_3 = \mu_3^{p} + RTln(1 - x)\gamma_3 + v_3(P - P_0), \quad (16)$$

where μ_3^{p} is pure water chemical potential. The strategy for calculating activity coefficient is given in Svandal et al. [21].

V. Results and Discussions

As an initial setup a structure I hydrate reservoir model is considered by inserting a thin water band between methane hydrate and CO2 liquid. This is a more realistic setup in comparison to the previous work [14]. The strip of water layer is shown as dark red strip around light red circular disk methane hydrate in Fig.2. This whole is then surrounded by CO2 liquid. It is believed that the CO2/CH4 exchange process will be faster due to higher diffusivity of CO2 in water and water in hydrate but all depends on the initial nucleation of CO2 hydrate on CO2 and water interface which is a very slow process. Therefore, four small regions of nucleation as CO2 hydrate of size 1Å×1Å are considered on the water and CO2 interface before running the simulation to let the things happen. These points are highlighted with white circles in Fig.2. The size of system is (150Å×150Å) with diameter of 60Å for circular hydrate. The temperature (276.15 K) and pressure (83.0 bar) remain constant in the system. The temperature and pressure condition is well inside the stability region of the guest molecules. The molar density of CO2 liquid is calculated using SRK equation of state. Hydrate density is calculated using the formulation by Sloan et al. [22].

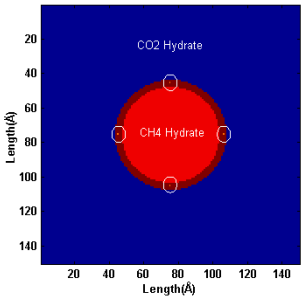

Fig.2 Initial picture of CH4 hydrate, water strip and liquid CO2 with 150Åx150Å size and a hydrate diameter of 60Å.

The simulation is run to 15.376 ns. The initial mole fraction of methane in hydrate is 0.14 is considered with the assumption that all small and large cavities are occupied by methane. Fig. 3 shows the initial density profile on the center line of the hydrate system passing through the hydrate. Many up-coming figures only show the profiles on the center line of the 2D-hydrate system passing through hydrate.

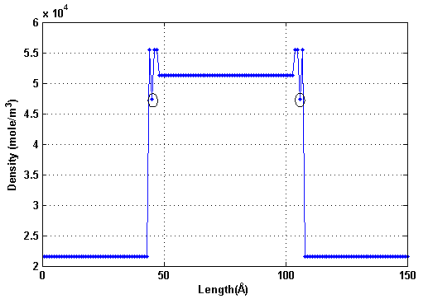

Fig.3 Density profile at time zero. Points encircled are the nucleation points and therefore CO2 hydrate density.

Methane hydrate initially starts to dissociate into the surrounding water. This is due to the driving force in terms of the change in chemical potential of methane in liquid phase and hydrate phase. This Phenomenon can be seen in Fig.4.

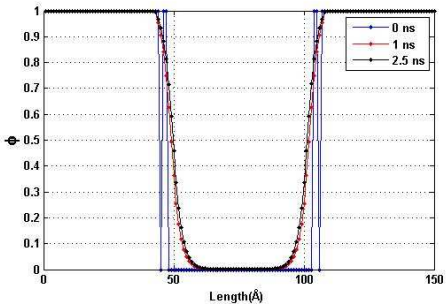

Fig.4. Phase Field parameter ϕ profile showing initial methane hydrate dissociation.

The CO2 starts penetrating into the methane hydrate as some empty spaces into the hydrate cavities are now available after some amount of methane has been released into the liquid phase. CO2 is assumed to only enter the large cavities of structure I due to its size. In Fig.5 both phase field parameter and CO2 profiles are plotted to exactly see the growth of CO2 in hydrate.

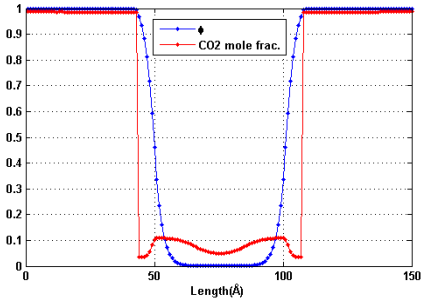

Fig.5. CO2 growth in methane hydrate at 2.5 ns.

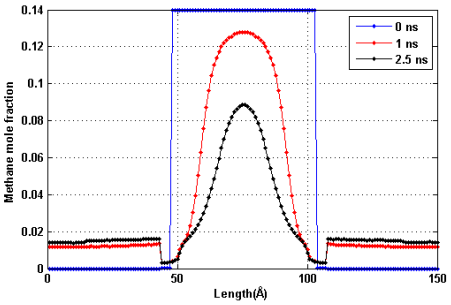

Fig.6. Methane drop inside hydrate and increase in surrounding with time.

Fig.6. shows the initial drop in methane concentration in hydrate. This is exactly can be seen in the methane flux profile in Fig.7. where dissolution rate drops quickly in first very few nano seconds.

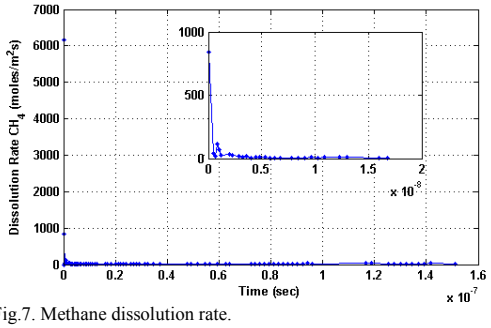

Fig.7. Methane dissolution rate.

To calculate the movement of methane from solid phase to liquid, the velocity on the interface is determined by tracking the ϕ values which is used to calculate the dissociation rate until 15.376 ns using the following equation from Sloan et al. [22]:

$$DR = SR \times \frac{\rho_{Hyd}}{M_G}\left(\frac{M_G}{M_G + 0.018 H_N}\right).$$

where DR is the dissociation rate (moles/m^{2}s), SR is hydrate radius shrinkage rate (m/s), ρ_{Hyd} is density of hydrate (kg/m^3), M_G is molar weight of the guest (kg/moles) and H_N is Hydrate number. The initial value of flux was high due to the initial relaxation of a system into a physically realistic interface.

Further, we give a figure (Fig.8) showing the mole fractions of methane and CO2 simultaneously. The figure shows mole fractions of both guests starts from the center to the wall of the system. Mole fractions of guests are given on three simulation times til 2.5 ns.

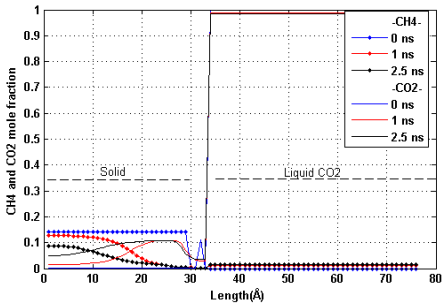

Fig.8. Methane and CO2 Mole fractions.

All these evidently shows that CO2 grows inside hydrate and the difference in chemical potentials inside and outside hydrate is the driving force while in similar way methane releases and leaving space for CO2.

Fig.9. shows direction arrows of velocity using velocity data in horizontal and vertical directions. The molecule movement outside the hydrate and towards the hydrate is clearly visible.

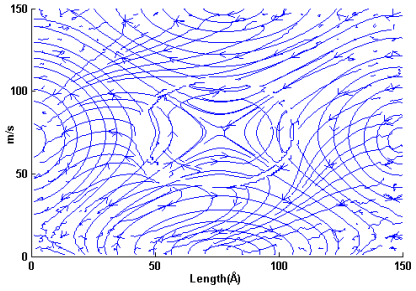

Fig.9. Direction arrows of flow at 2.5 ns.

The hydrate size is reduced because of methane dissociation until 2.5 nano seconds and then it start increasing till 12.57 ns due to reformation with CO2 penetration. This phenomenon is best explained by assistance of Fig.10, which illustrates the reformation process of CO2 hydrate, where the kinetics of the liquid CO2 from its liquid phase transformation to solid phase at different stages is plotted.

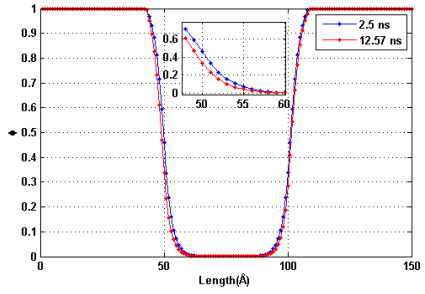

Fig.10. Hydrate reformation after initial dissociation due to CO2 penetration starting after 2.5 ns till 12.57 ns.

At the same time that is after 12.57 ns methane mole fraction also drops (see Fig.11) which initially was 0.14.

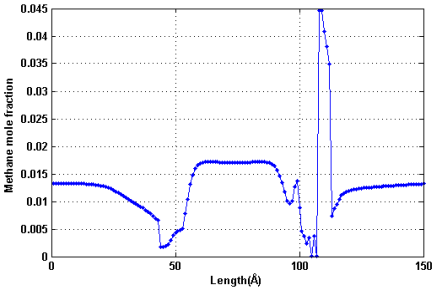

Fig.11. Methane mole fraction after 12.57 ns, drop in methane mole fraction is visible inside hydrate and increase elsewhere.

The in-out molecule movement is still continuing after 12.57 ns. A significant activity on the interface can still be observed. This can be observed by Fig.12 as well.

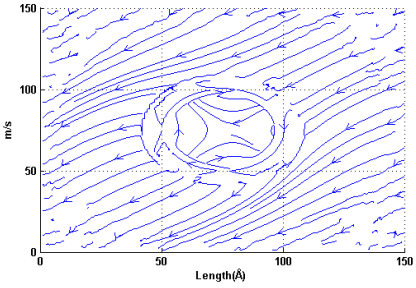

Fig.12. Flow profile after 12.57 ns, after full possible exchange.

The density profile is also transformed and after 12.57 ns the density of CO2 liquid drop as methane has penetrated and may have free gas in few places. This can be seen in Fig.13 and 14.

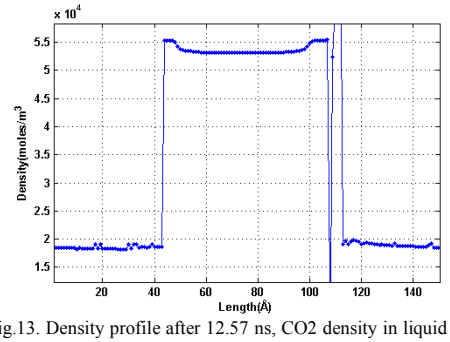

Fig.13. Density profile after 12.57 ns, CO2 density in liquid drops as methane has released after dissociation.

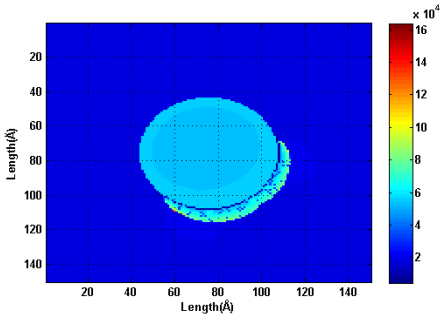

Fig.14. Density profile on whole 2D plane after 12.57 ns.

The increase of CO2 concentration inside hydrate is visible through Fig.15. The CO2 concentration is plotted along with Phase field parameter.

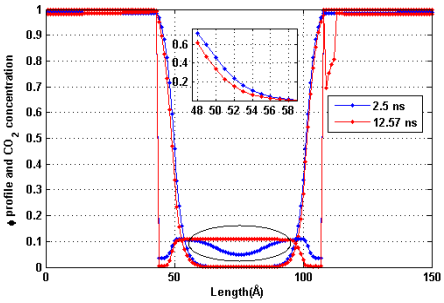

Fig.15. Combine plot of CO2 concentration and phase field parameter to see the hydrate reformation due to CO2 penetration in hydrate.

The area encircled clearly shows the growth of CO2 concentration inside hydrate and after 12.57 ns nearly 90 % of large cavities are filled with CO2. The hydrate at this time is not in stable condition and right after this time the hydrate starts dissociating again and in the matter of less than 3 ns the hydrate completely dissociates. The reason is the very low mole fraction of CO2 on the interface and access water. The CO2 exists in the range 0.3% to 0.8 % in water. Methane is even lower and is in the range of 0.1 % to 0.3 %. The corresponding chemical potential of CO2 in aqueous in the interface is from -3.2646E+04 j/mol to -3.4226E+04 j/mol respectively. On the other hand the mole fraction of CO2 inside the hydrate has raised up to 0.108 which means the chemical potential of CO2 in hydrate is -3.18450E+04 j/mol which is quite high then the chemical potential of CO2 in aqueous in the interface. This difference of free energy triggers the dissociation of hydrate. Fig. 16 gives a comparison of mole fractions of CO2 and water at 12.57 ns.

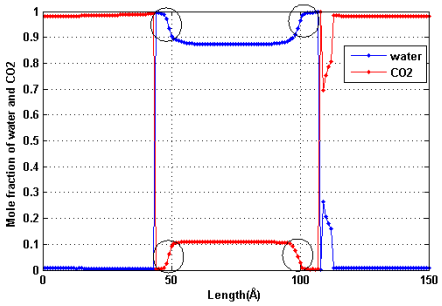

Fig.16. Water and CO2 mole fraction comparison after 12.57 ns.

The encircled regions shows a clearly that CO2 is very low in the interface in comparison to water. The methane is also very low in the same region as can be observed in Fig. 10. Once the dissociation starts the CO2 remain low as dissociation results more water and little CO2 to add in the interface. Fig. 17 clearly shows an even more drop in CO2 in interface after a very small time.

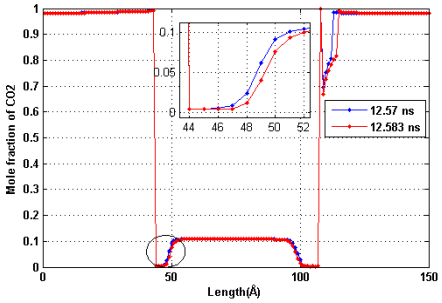

Fig. 17. CO2 mole fraction comparison 12.57 ns and 12.583 ns.

The encircled region is zoomed to clearly show the decrease in CO2 mole fraction in interface. On the other hand the water content grows more with time as suggested by Fig. 18.

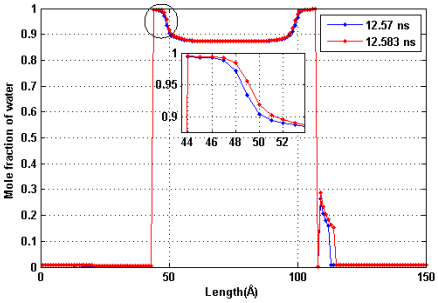

Fig. 18. Water mole fraction comparison 12.57 ns and 12.583 ns.

Again, the encircled region is zoomed to explain the growth of water on interface. This means that with time the CO2 drops and the water grows even more in interface and hence dissociation fasts with each passing time. That's the reason

why it results in a very rapid dissociation of the whole hydrate. For instance, the phase field parameter profiles are shown in Fig. 19 at 12.57 ns and 12.796 ns to show the rapid dissociation process.

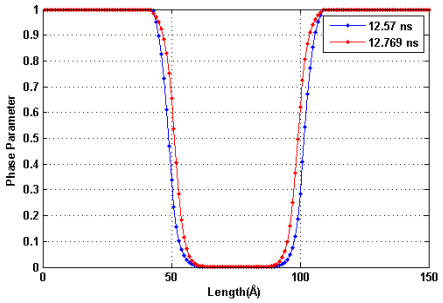

Fig. 19. Phase parameter comparison 12.57 ns and 12.769 ns.

The whole hydrate dissociates at 15.376 ns and phase parameter profile shows it in Fig. 20.

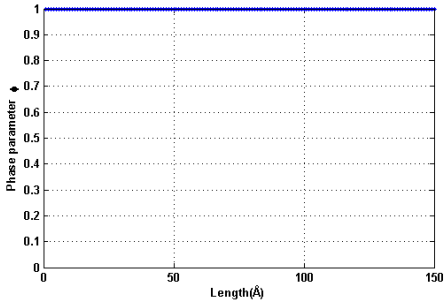

Fig. 20. Phase parameter at 15.376 ns showing full dissociation.

The CO2 and methane mole fractions are now very low in the previous hydrate region as expected, see Fig 21 and Fig.22.

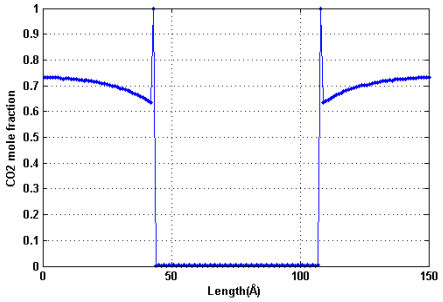

Fig.21. CO2 mole fraction after full dissociation.

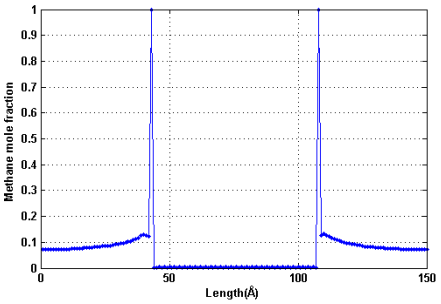

Fig.22. Methane mole fraction after full dissociation.

Phase field simulation with more appropriate description of thermodynamic model as well hydrodynamic [9] has been applied to model the exchange of CH4 with CO2 from natural gas hydrate at more realistic conditions corresponding to hydrates reservoir then in [14]. The data attained is useful in the modeling and optimization for the production of methane from hydrate reservoir as well as sequestration of CO2. As expected it was observed that the mole fraction of CO2 in the hydrate phase increases, while that of CH4 decreases with increasing time. It is also observed that the insertion of water band around methane hydrate speeds up the exchange process and hence CO2 hydrate reformation. After almost a 90 % exchange of CO2 with methane in large cavities the hydrate starts dissociating due to very low CO2 concentration in interface and high CO2 concentration inside the hydrate. The CO2 amount kept dropping during the dissociation and water kept rising on the interface which makes the dissociation very fast and in less than 3 ns the hydrates dissociates completely.

VI. Acknowledgment

This paper is a contribution to the Norwegian Research Council PETROMAKS project Gas hydrates on the Norwegian-Barents Sea-Svalbard margin (GANS, Norwegian Research Council Project No. 175969/S30).

References

[1] K. A. Kvenvolden, B. W. Rogers, "Gaia's breathglobal methane exhalations," Marine and Petroleum Geology, Vol.22, pp. 579-590, 2005.

[2] I. R. MacDonald, N. L. Guinasso, Jr. R. Sassen, J. M. Brooks, L. Lee, K. T. Scott, "Gas hydrate that breaches the sea floor on the continental slope of the Gulf of Mexico," pp. 699 – 702, 1994.

[3] G. Rehder, S. H. Kirby, W. B. Durham, L.A. Stern, E. T. Peltzer, J. Pinkston, P. G. Brewer, "Dissolution rates of pure methane hydrate and carbon-dioxide hydrate in undersaturated seawater at 1000-m depth," Geochimica et Cosmochimica Acta, Vol. 68, no. 2, pp. 285 – 292, 2004.

[4] A. V. Egorov, K. Crane, P. R. Vogt, A.N. Rozhkov, P. P. Shirshov, "Gas hydrates that outcrop on the sea floor: stability models," Geo-Marine Letters, Vol.19, pp. 68 – 75, 1999.

[5] A. Saji, H. Yoshida et al., "Fixation of carbondioxide by clathrate-hydrate," Energy Conversion and Management, Vol. 33, no. (5 – 8), pp. 643 – 649, 1992.

[6] A. Yamasaki, H. Teng et al., "CO2 hydrate formation in various hydrodynamics conditions," Gas Hydrates: Challenges for the Future, Vol. 912, pp. 235 – 245, 2002.

[7] J. W. Lee, M. K. Chun et al., "Phase equilibria and kinetic behavior of CO2 hydrate in electrolyte and porous media solutions: Application to

ocean sequestration CO2," Korean Journal of Chemical Engineering, Vol. 19, no. 4, pp. 673 – 678, 2002.
[8] T. Xu, J. A. Apps, K. Pruess, "Numerical simulation of CO2 disposal by mineral trapping in deep aquifers," Appl. Geochem., Vol. 19, pp. 917 – 936, 2004.
[9] M. Qasim, B. Kvamme, K. Baig, "Phase field theory modeling of CH4/CO2 gas hydrates in gravity fields," International Journal of Geology, Vol. 5, no. 2, pp. 48 – 52, 2011.
[10] K. Caldeira, M. E. Wickett, "Ocean model predictions of chemistry changes from carbon dioxide emissions to the atmosphere and ocean," J. Geophys. Res, pp. 110 – 112, 2005.
[11] A. A. Wheeler, W. J. Boethinger, G. B. McFadden, "Phase field model for isothermal phase transitions in binary alloys," Physical Review A, Vol. 45, pp. 7424 – 7439, 1992.
[12] B. Kvamme, A. Svandal, T. Buanes, T. Kuznetsova, "Phase field approaches to the kinetic modeling of hydrate phase transitions," AAPG Memoir, Vol. 89, pp. 758 – 769, 2009.
[13] A. Svandal, "Modeling hydrate phase transitions using mean field approaches," University of Bergen, pp. 1 – 37, 2006.
[14] M. Qasim, B. Kvamme, K. Baig, "Modeling dissociation and reformation of methane and carbon dioxide hydrate using Phase Field Theorey with implicit hydrodynamics," 7th International Conference on Gas Hydrates (ICGH 2011), Edinburgh, Scotland, United Kingdom, July 17 – 21, 2011.
[15] B. Kvamme, K. Baig, J. Bauman, P. H. Kivelä, "Thermodynamics and kinetic modeling of CH4/CO2 exchange in hydrates," 7th International Conference on Gas Hydrates (ICGH 2011), Edinburgh, Scotland, United Kingdom, July 17 – 21, 2011.
[16] G. Tegze, L. Gránásy, "Phase field simulation of liquid phase separation with fluid flow," Material science and engineering, vol. 413 – 414, pp. 418 – 422, 2005.
[17] M. Conti, "Density change effects on crystal growth from the melt," Physical Review, vol. 64, pp. 051601, 2001.
[18] M. Conti, M. Fermani, "Interface dynamics and solute trapping in alloy solidification with density change," Physical Review, vol. 67, pp. 026117, 2003.
[19] M. Conti, "Advection flow effects in the growth of a free dendrite," Physical Review, vol. 69, pp. 022601, 2004.
[20] K. Baig, M. Qasim, P. H. Kivelä, B. Kvamme, "Phase field theory modeling of methane fluxes from exposed natural gas hydrate reservoirs (in press)," American Institute of Physics, 2010.
[21] A. Svandal, T. Kuznetsova, B. Kvamme, "Thermodynamic properties and phase transitions in the H2O/CO2/CH4 system," Fluid Phase Equilibria, vol. 246, pp. 177 – 184, 2006.
[22] E. D. Sloan, C. A. Koh, "Clathrate hydrates of natural gases (3rd ed)," Boca Raton, FL: CRC Press, 2008.